Optical Field Enhancement by Strong Plasmon Interaction in Graphene Nanostructures

Sukosin Thongrattanasiri* and F. Javier García de Abajo†

IQFR-CSIC, Serrano 119, 28006 Madrid, Spain

(Received 27 August 2012; published 30 April 2013)

The ability of plasmons to enhance the electromagnetic field intensity in the gap between metallic nanoparticles derives from their strong optical confinement relative to the light wavelength. The spatial extension of plasmons in doped graphene has recently been shown to be boldly reduced with respect to conventional plasmonic metals. Here, we show that graphene nanostructures are capable of capitalizing such strong confinement to yield unprecedented levels of field enhancement, well beyond what is found in noble metals of similar dimensions (∼ tens of nanometers). We perform realistic, quantum-mechanical calculations of the optical response of graphene dimers formed by nanodisks and nanotriangles, showing a strong sensitivity of the level of enhancement to the type of carbon edges near the gap region, with armchair edges favoring stronger interactions than zigzag edges. Our quantum-mechanical description automatically incorporates nonlocal effects that are absent in classical electromagnetic theory, leading to over an order of magnitude higher enhancement in armchair structures. The classical limit is recovered for large structures. We predict giant levels of light concentration for dimers ∼200 nm, leading to infrared-absorption enhancement factors $\sim 10^8$. This extreme light enhancement and confinement in nanostructured graphene has great potential for optical sensing and nonlinear devices.

DOI: 10.1103/PhysRevLett.110.187401 PACS numbers: 78.67.Wj, 42.25.Bs, 73.20.Mf, 78.20.Ci

Metallic nanoparticles are capable of enhancing and confining the electromagnetic field under external illumination via the excitation of surface plasmons—the collective oscillations of conduction electrons [1]. The degree of confinement is strongly dependent on particle size, shape, composition, and relative arrangement [2]. In particular, metallic dimers can reach high levels of field enhancement for small separations and polarization across the gap [3–5]. This is a consequence of the strong coupling between the plasmons of individual particles, which produces plasmon hybridization accompanied by large frequency redshifts [6]. A tutorial explanation of the physics involved is provided in the Supplemental Material [7]. Because of these properties, localized plasmons find application to optical detection [8–12], single-molecule sensing [13–17], cancer therapy [18,19], drug delivery [20], improved photovoltaics [21,22], and catalysis [23,24].

Recently, doped graphene has emerged as a material capable of supporting plasmons with unprecedented levels of field confinement [25–27]. This has been confirmed by experimentally mapping the spatial distribution of graphene plasmons constrained to regions ∼40 times smaller than the free-space light wavelength [28,29]. Although two-dimensional electron gases of massive electrons have been widely studied [30,31], the massless nature of charge carriers in graphene presents specific characteristics that make its plasmons unique [32]. More precisely, graphene plasmons can be electrically tuned [33,34], while estimates based on the measured dc mobility predict smaller dissipation than in noble metals [35–37], although optical phonons produce additional losses above ∼0.2 eV photon energy [25]. The extreme level of plasmon confinement in graphene should translate into large field enhancement, the description of which involves nonclassical aspects for structures smaller than ∼20 nm [38], in contrast to noble metals, for which classical theory works down to sizes <10 nm [39].

In this Letter, we predict unprecedented levels of the optical field enhancement and energy concentration produced by strong interaction between the plasmons of neighboring graphene nanoislands. We report realistic, quantum-mechanical calculations for the field induced near illuminated graphene dimers obtained from the full random-phase approximation (RPA), using tight-binding electron wave functions as input [38]. Specifically, we study pairs of graphene nanodisks and nanotriangles separated by narrow gaps. We find that the plasmon enhancement is strongly influenced by the type of atomic edge structure near the gap region. In particular, armchair edges produce larger induced fields and energy concentration than zigzag edges. Quantum-mechanical effects play an important role for nanoislands of tens of nanometers in size [38], and they slowly fade out at larger sizes, thus converging towards the results of a classical electromagnetic description of the carbon material. Therefore, we use classical theory to study ∼100 nm structures, in which we find light-intensity enhancement factors $\sim 10^8$.

We present near-field calculations of graphene nanostructures, using a quantum-mechanical tight-binding description of the electronic structure and the RPA for the linear response (see Supplemental Material [7]). We show in Fig. 1 near-field intensity enhancement spectra at the center of graphene nanodisk dimers (solid curves, disk diameter $D = 20$ nm, carbon-to-carbon gap distance

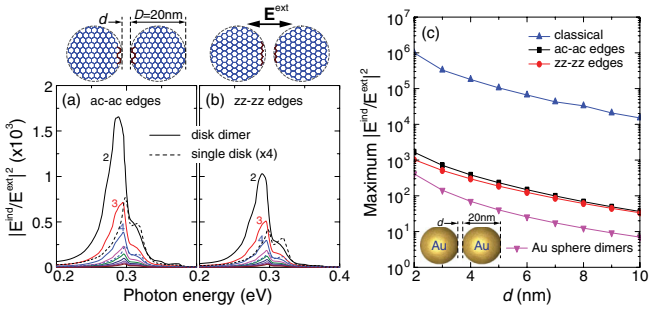

FIG. 1 (color online). Field enhancement in graphene nanodisk dimers. (a), (b) Electric-field intensity enhancement spectra at the center of nanodisk dimers (diameter $D = 20$ nm; see insets) for ac-ac (a) and zz-zz (b) gaps, as calculated in the RPA for normally incident light with polarization across the gap and edge-to-edge separations $d = 2, 3, \ldots, 10$ nm. Results for noninteracting nanoislands are given for comparison (broken curves for $d = 2$ and 4 nm). (c) RPA maximum electric-field intensity (black and red curves) compared with classical electromagnetic theory for graphene-disk (blue curve) and gold-sphere (purple curve) dimers of the same diameter. The graphene Fermi energy is $E_F = 0.4$ eV, and the intrinsic damping is $\hbar\tau^{-1} = 1.6$ meV throughout this work.

$d = 2$–10 nm). The incident electric field is across the gap. We consider two different relative orientations between the disks (see insets): armchair-to-armchair (ac-ac) [Fig. 1(a)] and zigzag-to-zigzag (zz-zz) [Fig. 1(b)]. Similar to conventional metal clusters [6], the plasmon field enhancement and redshift increase when d decreases. But in contrast to classical descriptions of these dimers, where Lorentzian shapes are expected [26], we find complex plasmon features with fine structure that is still resolvable for small cluster sizes. We attribute this effect to quantum confinement and nonlocality [38]. Additionally, the ac-ac dimers [Fig. 1(a)] produce substantially larger enhancement than the zz-zz dimers [Fig. 1(b)], as expected from the additional losses introduced by zz edges. The presence of zz edges reduces the enhancement compared with the prediction of a classical theory [see Fig. 1(c)].

We show for comparison results for noninteracting nanoislands [Figs. 1(a) and 1(b), broken curves], corresponding to 4 times the field intensity outside an individual nanodisk at a distance $d/2$ from its edge. A clear redshift is observed due to interaction (solid curves). Additionally, there is a twofold enhancement of the field intensity due to the interisland interaction (cf. solid and broken curves), in contrast to the far-field extinction, the strength of which is nearly unaffected by this interaction (see Supplemental Material [7]). Nonetheless, the field right outside an individual nanoisland is already substantially larger than what is obtained in conventional noble metal nanospheres of similar size.

Figure 1(c) shows the maximum field intensity as a function of d computed from classical (blue curve; see also Supplemental Material [7]) and quantum-mechanical (red and black curves) models. The former overestimates the enhancement, although our quantum-mechanical results show that these graphene nanostructures are performing significantly better than gold spheres of similar size (see purple curve and lower inset, obtained from a multiple-scattering approach [40] using tabulated optical data for the gold dielectric function [41]).

Given the damaging effect of zz edges, we consider structures in which only ac edges are present. Specifically, we focus on ac-ac bowties [Fig. 2(a)], which we compare with pure zz edge structures [Fig. 2(b)]. Near-zero-energy (NZE) electronic states are found in zz edges [42,43], which open new channels of plasmon decay [38]. In contrast, NZE states are not present in pure ac edge structures, such as the triangular bowties of Fig. 2(a). We compare the near-field intensity-enhancement spectra at the center of bowties in Figs. 2(a) and 2(b) for ac-ac and zz-zz configurations (see upper insets). Here, the triangle side length is fixed to

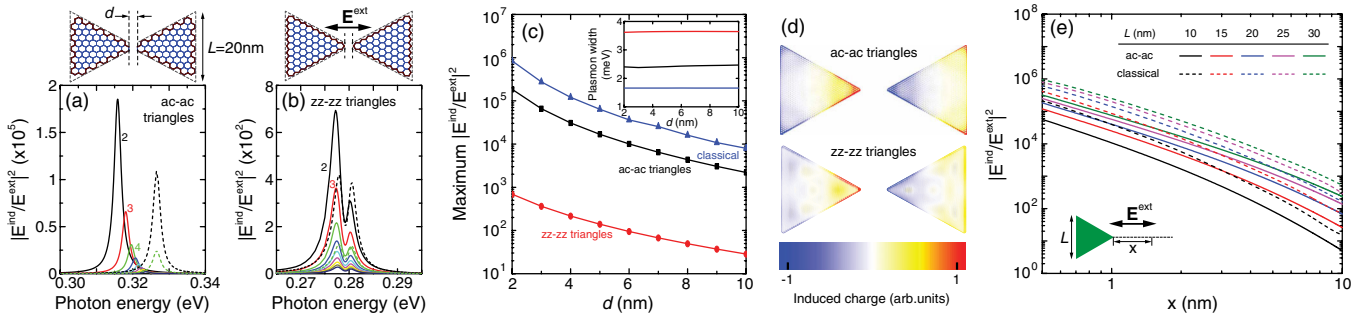

FIG. 2 (color online). Field enhancement in graphene bowties. (a), (b) Electric-field intensity enhancement spectra of nontouching bowties for gap distances $d = 2, 3, \ldots, 10$ nm. The graphene triangles have ac edges in (a) and zz edges in (b) (see upper insets). The triangle side length is $L = 20$ nm in all cases. Results for noninteracting nanoislands are shown for comparison (broken curves for $d = 2$ and 4 nm). (c) Maximum electric-field intensity at the gap center as a function of gap distance. The inset shows the plasmon width, as resolved from the extinction cross section (see Supplemental Material [7]). (d) Amplitude of the resonance induced-charge density for $d = 6$ nm (linear scale). (e) Dependence of the resonant intensity enhancement calculated both from the quantum-mechanical RPA (solid curves) and from classical electrodynamics (broken curves) as a function of distance from the corner of a single nanotriangle (see inset) for different values of the side length L (see labels).

$L = 20$ nm. Several striking differences between both types of structures are worth noticing: (i) ac-ac bowties produce field enhancement factors nearly 2 orders of magnitude higher than zz-zz bowties; (ii) the intertriangle interaction in ac-ac bowties is stronger, as evidenced by the larger plasmon redshift observed for decreasing gap distance; (iii) like in the nanodisks, the interisland interaction produces additional field enhancement and plasmon redshift [cf. solid and broken curves in Figs. 2(a) and 2(b)]; and (iv) the plasmon is split into two dominant features in both the individual and dimer zz configurations, of very different weight in the near field but of comparable weight in the extinction cross section (see Supplemental Material [7]); as a whole, the plasmonic strength is diluted into a wider spectral region, and this effect is dramatic when examining the extinction cross section (see Supplemental Material [7]). Incidentally, the influence of the gap distance and the type of edges is less dramatic on the cross section, as it is a far-field property (see Supplemental Material [7]).

The maximum field enhancement at the gap center is shown in Fig. 2(c) for both types of bowties and compared with the results of a classical description of the graphene (see Supplemental Material [7]). Interestingly, ac-ac bowties produce field enhancement factors 2 orders of magnitude larger than what we obtained for nanodisks and almost reaching the values predicted by classical theory. In contrast, zz-zz dimers show a modest level of enhancement. As shown in the inset, the field enhancement appears to decrease with increasing plasmon width. The latter is rather insensitive to the gap distance. This result is again consistent with our interpretation of losses in zz-zz bowties mainly coming from NZE states, with no significant effect due to the gap. Interestingly, the maximum enhancement exhibits a similar dependence on gap distance in all bowties. However, the decay with increasing distance is faster than that in the nanodisks of Fig. 1, which is understandable from the larger degree of mode localization in the gap of bowties.

The modes under consideration have a dipole-dipole structure, as illustrated by the induced charge densities represented in Fig. 2(d) for $d = 6$ nm, also showing large induced charges in ac-ac dimers compared with zz-zz dimers. Higher order modes do not couple strongly to light, as we discuss in detail in the Supplemental Material [7]. Interestingly, the induced charges are abundantly localized at the edges of the ac triangles, but they spatially oscillate along the central regions of the zz triangles.

The above quantum-mechanical description of the optical response of small graphene dimers (tens of nanometers) produces tremendously enhanced near-field intensities, particularly in ac-ac bowties. Interestingly, classical theory is far from these results, despite the fact that the graphene sizes under consideration are already at the limit of the capabilities of currently available computers to deal with the optical response from first principles, and, therefore, it is difficult to perform a complete analysis of the transition between quantum and classical regimes as the distance increases. However, the RPA is reasonably close to classical theory in ac-ac bowties, which produce the highest levels of enhancement, and therefore, we concentrate on these types of dimers. We further explore the convergence from the quantum to the classical regimes in Fig. 2(e) by representing the enhancement near individual ac nanotriangles of increasing size. The nonlocal effects captured in the RPA systematically lead to small values compared with the classical model. Closer examination reveals a slow reduction of quantum-mechanical effects with increasing x and L. This deviation from classical to quantum results is less than a factor of 5, and thus, we rely on classical theory to describe larger graphene structures, keeping in mind that a more realistic quantum-mechanical description might produce a field enhancement that is smaller by a factor of <5.

Since we are in the electrostatic limit (geometrical size $\ll$ free-space wavelength), larger sizes with similar gap distances must produce stronger field enhancement due to the reduction of the gap-to-size ratio. This is clearly shown in Fig. 3 for dimers consisting of nontouching ($d > 0$) and overlapping ($d < 0$) disks ($D = 100$ nm) and triangles ($L = 50$ nm). The gap-plasmon energy exhibits a nonsingular transition between touching and nontouching regimes, as expected from previous studies of gold dimers [5]. Likewise, the electric-field intensity enhancement is remarkably strong near this transition, reaching levels $\sim 10^8$, well above what is found in gold spheres. Surprisingly, the enhancement factor of the overlapping triangles is substantially smaller than the nonoverlapping geometry for similar values of d, presumably because the wedge formed after touching is wide, unlike what happens in disks and sphere dimers. We stretch again that these results for disks might undergo severe downwards corrections due to nonlocal effects (e.g., the emergence of new junction plasmon modes in narrow graphene bridges [44]), whereas bowties with armchair edges should behave close to the classical results presented in Fig. 3(b). Incidentally, the enhancement produced at the center of the gap when we dismiss the interaction between separate disks [Fig. 3(a), dashed curve, barely visible near $d = 0$] and triangles [Fig. 3(b), dashed curve] is substantially reduced, and thus, the gap enhancement effect is rather strong for large size-to-gap ratios.

The unprecedented levels of field enhancement shown here originate in the combination of two effects: (i) the large field confinement of plasmons in this carbon material [25–27] and (ii) the additional confinement brought about by narrow gaps [5]. The enhancement factor is largely influenced by the kind of carbon edge terminations near the gap region and the abundance of zigzag edges in the rest of the structure. Specifically, zigzag edges limit the degree of field enhancement in the gap and produce plasmon broadening by introducing additional loss channels

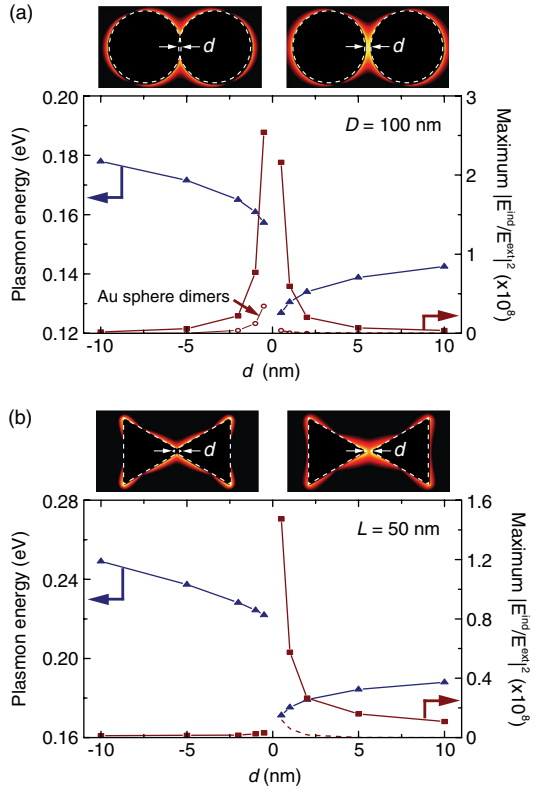

FIG. 3 (color online). Giant plasmon field enhancement in large graphene nanodimers. Plasmon energy (left scale) and resonant field enhancement at the gap center (right scale) in dimers formed by graphene disks [(a), diameter $D = 100$ nm] and triangles [(b), side length $L = 50$ nm] as a function of gap distance d, calculated from classical theory. Negative d values correspond to overlapping structures. Results for gold-sphere dimers are plotted in (a) for comparison (open symbols, sphere diameter equal to 100 nm). The insets show electric near-field intensity maps for $d = -5$ and $d = 5$ nm.

connected to the existence of near-zero-energy gap states [38,45]. For structures of tens of nanometers in size, the electric-field intensity enhancement reaches 10^5 at separations of 2 nm in bowties fully terminated with armchair edges. The enhancement is less pronounced in zigzag bowties and in nanodisk dimers, which contain a mix of both types of edge terminations. The quantum-mechanical calculations converge to the classical electromagnetic description as the carbon cluster size increases. For 100 nm nanoislands, classical theory predicts an intensity enhancement of $\sim 10^8$.

In our calculations, the maximum field amplitude is roughly proportional to the impurity- and phonon-limited intrinsic lifetime $\tau \approx 400$ fs (see Supplemental Material [7]), which we estimate from moderate measured dc mobilities [35,36]. Impurities in lower-quality graphene can reduce τ by 1 order of magnitude [46], and thus, the challenge is to produce high quality samples, which have been shown to yield mobilities a factor of 10 larger than what we are assuming throughout this work [37,47]. Additionally, optical phonons contribute to decoherence for energies above 0.2 eV and can produce a slight correction to our effective value of τ [25]. Furthermore, electron-electron interactions (here described within the RPA approximation), as well as edge and finite-size effects, contribute to plasmon decoherence [38], and they are appropriately accounted for in our tight-binding RPA description, producing extra broadening to the plasmon features compared to the classical description (see Supplemental Material [7] for a more detailed discussion), particularly in small structures (tens of nanometers) with zigzag edges. In contrast, the lifetime in armchair bowties is dominated by the intrinsic value of τ (see Supplemental Material [7]).

The reported strong near-field enhancement could drive nanoscale highly nonlinear response either in nearby materials or in the graphene itself, which displays large second- and third-order nonlinearities [48–51]. Likewise, a strong field confinement can be used to increase the intensity of molecule-specific optical scattering (e.g., via infrared absorption), particularly in the infrared part of the spectrum. Interestingly, the field enhancement near individual nanoislands is already remarkably high, which is advantageous from the fabrication point of view. Importantly, these exciting properties take place at frequencies that can be selected by chemically [52] or electrically [28,29,46] changing the doping conditions. The mediation of doped graphene nanostructures such as those considered here is thus a promising strategy for producing new optical sensing and nonlinear tunable devices, particularly in view of the latest advances in the controlled fabrication of graphene structures with subnanometer detail [53].

This work has been supported in part by the Spanish MEC (Grant No. MAT2010-14885 and Consolider NanoLight.es) and Ibercivis.

*sukosin@gmail.com
†J.G.deAbajo@nanophotonics.es

[1] K. R. Li, M. I. Stockman, and D. J. Bergman, Phys. Rev. Lett. **91**, 227402 (2003).
[2] V. Myroshnychenko, J. Rodríguez-Fernández, I. Pastoriza-Santos, A. M. Funston, C. Novo, P. Mulvaney, L. M. Liz-Marzán, and F. J. García de Abajo, Chem. Soc. Rev. **37**, 1792 (2008).
[3] P. E. Batson, Ultramicroscopy **9**, 277 (1982).
[4] H. Xu, E. J. Bjerneld, M. Käll, and L. Börjesson, Phys. Rev. Lett. **83**, 4357 (1999).
[5] I. Romero, J. Aizpurua, G. W. Bryant, and F. J. García de Abajo, Opt. Express **14**, 9988 (2006).
[6] P. Nordlander, C. Oubre, E. Prodan, K. Li, and M. I. Stockman, Nano Lett. **4**, 899 (2004).
[7] See Supplemental Material at http://link.aps.org/supplemental/10.1103/PhysRevLett.110.187401 for further details on the calculation methods, additional numerical results, a discussion of mode symmetry, and a

tutorial explanation of optical field enhancement in dimers.
[8] A. McFarland and R. Van Duyne, Nano Lett. **3**, 1057 (2003).
[9] A. B. Dahlin, J. O. Tegenfeldt, and F. Höök, Anal. Chem. **78**, 4416 (2006).
[10] K.-S. Lee and M. A. El-Sayed, J. Phys. Chem. B **110**, 19 220 (2006).
[11] M. E. Stewart, C. R. Anderton, L. B. Thompson, J. Maria, S. K. Gray, J. A. Rogers, and R. G. Nuzzo, Chem. Rev. **108**, 494 (2008).
[12] J. N. Anker, W. P. Hall, O. Lyandres, N. C. Shah, J. Zhao, and R. P. Van Duyne, Nat. Mater. **7**, 442 (2008).
[13] S. Nie and S. R. Emory, Science **275**, 1102 (1997).
[14] K. Kneipp, Y. Wang, H. Kneipp, L. T. Perelman, I. Itzkan, R. R. Dasari, and M. S. Feld, Phys. Rev. Lett. **78**, 1667 (1997).
[15] P. Johansson, H. Xu, and M. Käll, Phys. Rev. B **72**, 035427 (2005).
[16] C. E. Talley, J. B. Jackson, C. Oubre, N. K. Grady, C. W. Hollars, S. M. Lane, T. R. Huser, P. Nordlander, and N. J. Halas, Nano Lett. **5**, 1569 (2005).
[17] L. Rodríguez-Lorenzo, R. A. Álvarez-Puebla, I. Pastoriza-Santos, S. Mazzucco, O. Stéphan, M. Kociak, L. M. Liz-Marzán, and F. J. García de Abajo, J. Am. Chem. Soc. **131**, 4616 (2009).
[18] X. Qian, X.-H. Peng, D. O. Ansari, Q. Yin-Goen, G. Z. Chen, D. M. Shin, L. Yang, A. N. Young, M. D. Wang, and S. Nie, Nat. Biotechnol. **26**, 83 (2008).
[19] L. Hirsch, R. Stafford, J. Bankson, S. Sershen, B. Rivera, R. Price, J. Hazle, N. Halas, and J. West, Proc. Natl. Acad. Sci. U.S.A. **100**, 13 549 (2003).
[20] Y. L. Luo, Y. S. Shiao, and Y. F. Huang, ACS Nano **5**, 7796 (2011).
[21] K. R. Catchpole and A. Polman, Opt. Express **16**, 21 793 (2008).
[22] H. A. Atwater and A. Polman, Nat. Mater. **9**, 205 (2010).
[23] R. Asahi, T. Morikawa, T. Ohwaki, K. Aoki, and Y. Taga, Science **293**, 269 (2001).
[24] P. V. Kamat, J. Phys. Chem. B **106**, 7729 (2002).
[25] M. Jablan, H. Buljan, and M. Soljačić, Phys. Rev. B **80**, 245435 (2009).
[26] F. H. L. Koppens, D. E. Chang, and F. J. García de Abajo, Nano Lett. **11**, 3370 (2011).
[27] A. Y. Nikitin, F. Guinea, F. J. García-Vidal, and L. Martín-Moreno, Phys. Rev. B **84**, 195446 (2011).
[28] J. Chen *et al.*, Nature (London) **487**, 77 (2012).
[29] Z. Fei *et al.*, Nature (London) **487**, 82 (2012).
[30] F. Stern, Phys. Rev. Lett. **18**, 546 (1967).
[31] I. V. Kukushkin, D. V. Kulakovskiĭ, S. A. Mikhaĭlov, J. H. Smet, and K. von Klitzing, JETP Lett. **77**, 497 (2003).
[32] W. Wang, P. Apell, and J. Kinaret, Phys. Rev. B **84**, 085423 (2011).
[33] L. Ju *et al.*, Nat. Nanotechnol. **6**, 630 (2011).
[34] S. Thongrattanasiri, I. Silveiro, and F. J. García de Abajo, Appl. Phys. Lett. **100**, 201105 (2012).
[35] K. S. Novoselov, A. K. Geim, S. V. Morozov, D. Jiang, Y. Zhang, S. V. Dubonos, I. V. Grigorieva, and A. A. Firsov, Science **306**, 666 (2004).
[36] K. S. Novoselov, A. K. Geim, S. V. Morozov, D. Jiang, M. I. Katsnelson, I. V. Grigorieva, S. V. Dubonos, and A. A. Firsov, Nature (London) **438**, 197 (2005).
[37] K. I. Bolotin, K. J. Sikes, Z. Jiang, M. Klima, G. Fudenberg, J. Hone, P. Kim, and H. L. Stormer, Solid State Commun. **146**, 351 (2008).
[38] S. Thongrattanasiri, A. Manjavacas, and F. J. García de Abajo, ACS Nano **6**, 1766 (2012).
[39] J. A. Scholl, A. L. Koh, and J. A. Dionne, Nature (London) **483**, 421 (2012).
[40] F. J. García de Abajo, Phys. Rev. B **60**, 6086 (1999).
[41] P. B. Johnson and R. W. Christy, Phys. Rev. B **6**, 4370 (1972).
[42] A. R. Akhmerov and C. W. J. Beenakker, Phys. Rev. B **77**, 085423 (2008).
[43] M. Wimmer, A. R. Akhmerov, and F. Guinea, Phys. Rev. B **82**, 045409 (2010).
[44] S. Thongrattanasiri, A. Manjavacas, P. Nordlander, and F. J. García de Abajo, Laser Photonics Rev. **7**, 297 (2013).
[45] A. Manjavacas, S. Thongrattanasiri, and F. J. García de Abajo, Nanophotonics **2**, 139 (2013).
[46] Z. Q. Li, E. A. Henriksen, Z. Jian, Z. Hao, M. C. Martin, P. Kim, H. L. Stormer, and D. N. Basov, Nat. Phys. **4**, 532 (2008).
[47] C. R. Dean *et al.*, Nat. Nanotechnol. **5**, 722 (2010).
[48] S. A. Mikhailov, Europhys. Lett. **79**, 27002 (2007).
[49] E. Hendry, P. J. Hale, J. Moger, A. K. Savchenko, and S. A. Mikhailov, Phys. Rev. Lett. **105**, 097401 (2010).
[50] S. A. Mikhailov, Phys. Rev. B **84**, 045432 (2011).
[51] A. E. Nikolaenko, N. Papasimakis, E. Atmatzakis, Z. Q. Luo, Z. X. Shen, F. de Angelis, S. A. B. E. di Fabrizio, and N. I. Zheludev, Appl. Phys. Lett. **100**, 181109 (2012).
[52] C. F. Chen *et al.*, Nature (London) **471**, 617 (2011).
[53] F. Börrnert, L. Fu, S. Gorantla, M. Knupfer, B. Büchner, and M. H. Rümmeli, ACS Nano **6**, 10 327 (2012).